

DISCOVERY OF BLUE LUMINESCENCE IN THE RED RECTANGLE: POSSIBLE FLUORESCENCE FROM NEUTRAL POLYCYCLIC AROMATIC HYDROCARBON MOLECULES?

UMA P. VIJH,^{1,2} ADOLF N. WITT,^{1,2} AND KARL D. GORDON³

Received 2003 December 1; accepted 2004 March 19; published 2004 April 5

ABSTRACT

Here we report our discovery of a band of blue luminescence (BL) in the Red Rectangle nebula. This enigmatic proto-planetary nebula is also one of the brightest known sources of extended red emission as well as of unidentified infrared (UIR) band emissions. The spectrum of this newly discovered BL is most likely fluorescence from small neutral polycyclic aromatic hydrocarbon (PAH) molecules. PAH molecules are thought to be widely present in many interstellar and circumstellar environments in our Galaxy as well as in other galaxies and are considered likely carriers of the UIR band emission. However, no specific PAH molecule has yet been identified in a source outside the solar system because the set of mid-infrared emission features attributed to these molecules between the wavelengths of 3.3 and 16.4 μm is largely insensitive to molecular sizes. In contrast, near-UV/blue fluorescence of PAHs is more specific as to size, structure, and charge state of a PAH molecule. If the carriers of this near-UV/blue fluorescence are PAHs, they are most likely neutral PAH molecules consisting of three to four aromatic rings such as anthracene ($\text{C}_{14}\text{H}_{10}$) and pyrene ($\text{C}_{16}\text{H}_{10}$). These small PAHs would then be the largest molecules specifically identified in the interstellar medium.

Subject headings: ISM: individual (Red Rectangle) — ISM: molecules — radiation mechanisms: general

On-line material: color figures

1. INTRODUCTION

The family of emission bands at 3.3, 6.2, 7.7, 8.6, 11.2, and 12.7 μm (called the unidentified infrared [UIR] bands) is found in almost all astrophysical environments, including the diffuse interstellar medium (ISM), the edges of molecular clouds, reflection nebulae, young stellar objects, H II regions, star-forming regions, some C-rich Wolf-Rayet stars, post-asymptotic giant branch (AGB) stars, planetary nebulae, novae, normal galaxies, starburst galaxies, most ultraluminous infrared galaxies, and active galactic nuclei (see Peeters et al. 2004 and references therein). Approximately 20%–30% of the Galactic IR radiation is emitted in these UIR bands, and 10%–15% of the interstellar carbon is contained in the UIR carriers (Snow & Witt 1995), indicating that the carriers represent an abundant component of the ISM. These UIR bands are the signatures of aromatic C-C and C-H fundamental vibrational and bending modes and are generally attributed to a family of polycyclic aromatic hydrocarbon (PAH) molecules containing 50–100 carbon atoms (Hony et al. 2001; Cook & Saykally 1998; Leger & Puget 1984; Verstraete et al. 2001; Allamandola, Tielens, & Barker 1985; Sellgren 1984). Although the presence of PAHs in space is widely accepted by most astronomers, their specific sizes and ionization states remain elusive. On absorption of a far-UV photon, a PAH molecule usually undergoes a transition to an upper electronic state. If the molecule undergoes iso-energetic transitions to highly vibrationally excited levels of the ground state, then the molecule relaxes through a series of IR emissions in the C-C and C-H vibrational and bending modes. These transitions are largely independent of size, structure, and ionization state of the molecule. However, *electronic*

fluorescence, a transition from the upper excited level to the ground state, is more specific (Reylé & Bréchnignac 2000). In particular, the wavelength of the first electronic transition in neutral PAHs is closely dependent on the size of the molecular species. In general, this fluorescence wavelength increases with the molecular weight of the molecule (Fig. 1). An observation of fluorescence in an astronomical source in the UV/visible range offers the possibility of estimating the size of the PAH molecules; the observation of the UIR band emission in the same source does not.

2. TARGET AND OBSERVATIONS

The Red Rectangle (RR; Cohen et al. 1975; van Winckel 2003) is a unique proto-planetary nebula. Its bipolar structure is a result of mass loss from an evolved central binary star, HD 44179, directed by a circumbinary disk. Different aspects of the nebula become apparent in images at different wavelength regions shown in Figure 2. At blue wavelengths ($3800 \text{ \AA} < \lambda < 4900 \text{ \AA}$, *bottom panel*), the nebular structure is dominated by a bright spherical blob of about 8" diameter, embedded in a faint rectangular envelope with approximate dimensions of $12'' \times 24''$. The blue spectrum of the nebula is dominated by dust-scattered light of the central A-type star. At red wavelengths (6220 \AA), the nebula appears to have sharp radial structures, representing the projected walls of a biconical outflow cavity, as shown in the high-resolution *Hubble Space Telescope* (HST) Wide Field Planetary Camera 2 (WFPC2) image in the middle panel. The nebular spectrum in the red region ($\lambda > 5400 \text{ \AA}$) is dominated by extended red emission (ERE; Witt & Vjih 2004; Witt & Boroson 1990), following a spatial distribution (Schmidt & Witt 1991) totally different from that of the dust-scattered light at blue wavelengths ($\lambda < 5000 \text{ \AA}$). The carrier of the ERE is still under investigation (Witt & Vjih 2004). The top panel shows a high-resolution short-exposure WFPC2 near-IR image of the central source, demonstrating in fact that the star itself is not directly visible from Earth. Instead, we

¹ Ritter Astrophysical Research Center, University of Toledo, 2801 West Bancroft Street, Toledo, OH 43606.

² Visiting Astronomer, Cerro Tololo Inter-American Observatory (CTIO), which is operated by AURA, Inc., under contract to the National Science Foundation.

³ Steward Observatory, University of Arizona, 933 North Cherry Avenue, Tucson, AZ 85721-0065.

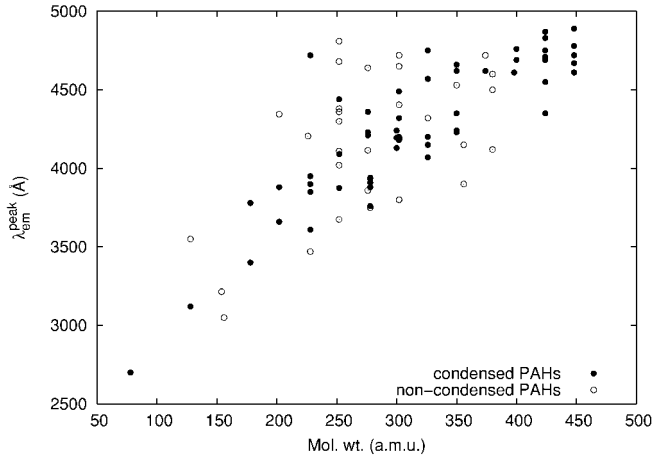


FIG. 1.—First electronic transition in the fluorescence spectra (Berlman 1965; Peaden et al. 1980; Ewald & Garrigues 1985; Ewald & Garrigues 1988) of neutral PAH molecules as a function of their molecular weight. We distinguish between condensed and noncondensed PAHs, with condensed PAHs considered to be more stable under interstellar conditions. [See the *electronic edition of the Journal for a color version of this figure.*]

see two blobs of scattered light above and below a disk (Bujarrabal et al. 2003), which obscures the star at visible wavelengths.

The RR nebula has the distinction of being the brightest known source of UIR band emission (Russell, Soifer, & Willner 1978; Geballe et al. 1985), which is attributed to PAHs. The central star HD 44179 is thought to be a post-AGB star in its first stage of evolution toward a planetary nebula. It is in this stage that substantial mass loss takes place and that a bipolar structure develops. This stage in stellar evolution is considered a stage of active dust production (Whittet 2003). Therefore, the RR nebula is a likely location in which to find observational evidence of small PAH molecules, which are the building blocks for larger PAH structures (Keller 1987) and carbon grains. In most other sources of UIR band emission, the emitting particles are a component of *interstellar* dust, which is likely to have experienced substantial processing by UV radiation, interstellar shocks, and chemical modification over a very long time span of existence since leaving the environment of its original formation. It is well established that PAH molecules with less than 40 C atoms are unlikely to survive the harsh radiation conditions of interstellar space (Jochims, Baumgaertel, & Leach 1999), while they may well be abundant in the more benign, UV-poor radiation field of HD 44179, especially when partially shielded by the opaque disk apparent in Figure 2.

We obtained low-resolution, long-slit spectra of the RR with the Ritchey-Chrétien (Cassegrain) spectrograph at the CTIO 1.5 m telescope. These observations were made on 2003 March 26 using a 2"5 wide slit, 7'7 long. The grating 09 with 300 lines mm^{-1} , blazed at 4000 Å, provided a 8.6 Å resolution and a spectral coverage of 2600 Å. Using a CuSO_4 filter to select the grating's first order, the setup covered a wavelength range of 3400–6000 Å, including the range from $\text{H}\beta$ to the Balmer discontinuity. The Loral IK CCD detector yielded a spatial scale of 1"3 pixel^{-1} along the slit. We used a coronagraphic decenter assembly to minimize scattered light from the star while probing as much of the inner nebula as possible. All observations were made using the full extent of the 7'7 long slit to get simultaneous sky observations. We obtained spectra at two nebular locations, 2"5 and 5" south of the central star HD 44179 with the slit in

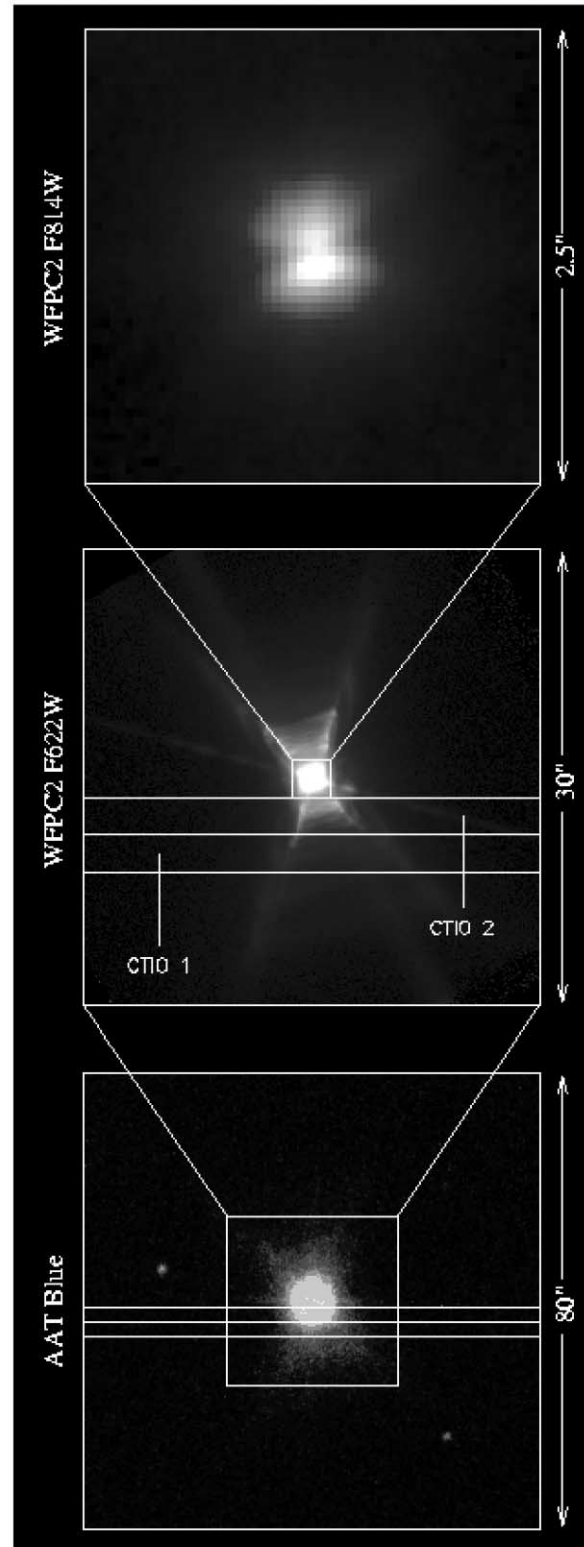


FIG. 2.—RR nebula. These images illustrate the observable structures of the RR nebula at different optical wavelengths and different angular scales. The bottom panel shows a blue image (3800–4900 Å), obtained using the 4 m Anglo-Australian Telescope (AAT). The middle panel shows an *HST* WFPC2 image centered at a wavelength of 6220 Å. The geometry of the central illuminating source, obscured from direct visibility by an optically opaque circumstellar disk, is shown in the top panel, obtained with the *HST* WFPC2 at a wave band centered at 8140 Å. The angular scales of each of the three frames are indicated on their right-hand sides. The orientation and width of the two CTIO spectrograph slits are indicated on both the bottom and middle panels and are labeled CTIO 1 and CTIO 2, respectively. [See the *electronic edition of the Journal for a color version of this figure.*]

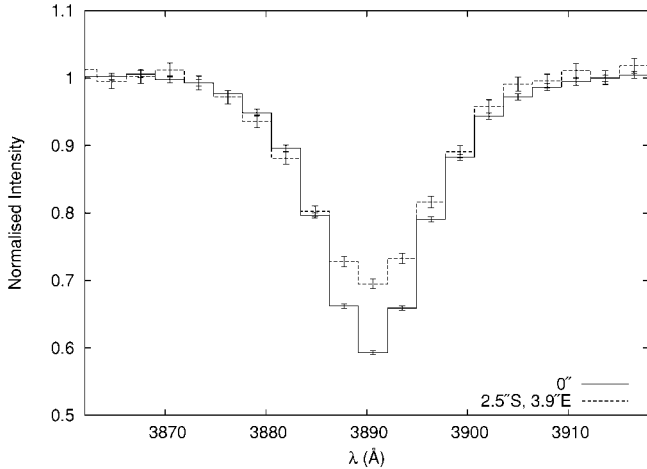


FIG. 3.—Normalized spectra from two positions, zero offset and 2.5 south, 3.9 east at 3889 Å, illustrating the filling in of the Balmer line due to fluorescence. Error bars are photon-statistics errors.

the east-west direction. The nebular exposures were bracketed by exposures of the central star. Individual exposures were limited to 5–10 minutes on the nebula and 1 minute for the star, and four to five exposures were obtained for each orientation. Data reductions were carried out with IRAF 2.12 EXPORT, and all spectra were flux-calibrated via the observation of standard stars.

3. RESULTS

3.1. Line-Depth Technique

We used the line-depth technique to initially detect and measure the fluorescence spectrum at each of the two nebular positions. This technique allows us to identify and measure any continuous emission in a reflected spectrum, such as represented by the blue spectrum of the RR, relying on the comparison of the depths of nebular and stellar spectral absorption lines. It works particularly well with the strong hydrogen Balmer lines at 6562, 4861, 4340, 4101, 3970, 3889, 3835, 3798, 3770 Å, In the absence of any emission processes such as continuous fluorescence by PAH molecules, the relative line depths in the reflected spectrum would be identical to the corresponding ones in the spectrum of the illuminating star, assuming that the wavelength-dependent scattering properties of the dust, e.g., albedo and phase function asymmetry, remain unchanged over the few-angstrom width of each individual line. The presence of any continuous emission manifests itself by the lines in the reflected spectrum having smaller line depths than those in the illuminating source spectrum. The illuminating source in this case is the star HD 44179, having an ideal spectral type A with strong Balmer lines. Also, at $T_{\text{eff}} \leq 9000$ K, the star is not likely to produce Balmer line emission in the surrounding nebula. The decrease in the depth of a line can be directly related to the amount of underlying continuous emission (in this case, the fluorescence intensity). As the star is enshrouded by the disk and as the stellar spectrum is actually seen in reflected light, if there were any fluorescence in this zero-offset spectrum, the line-depth technique would reveal any additional fluorescence at the offset positions in the nebula.

As an example, we show in Figure 3 the normalized spectra at the zero-offset position and at an offset 2.5 south, 3.9 east of H ζ at 3889 Å. One can see that the line depth at the nebular position is substantially diminished.

TABLE 1
FLUORESCENCE INTENSITY AT TWO POSITIONS IN THE RR NEBULA

WAVELENGTH (Å)	INTENSITY (ergs cm ⁻² s ⁻¹ Å ⁻¹ sr ⁻¹)	
	2.5 South, 3.9 East	5" South, 6.5 East
4861.3	$(4.059 \pm 0.026) \times 10^{-6}$	$(9.528 \pm 0.145) \times 10^{-8}$
4340.5	$(1.209 \pm 0.008) \times 10^{-5}$	$(1.571 \pm 0.025) \times 10^{-6}$
4101.7	$(2.914 \pm 0.020) \times 10^{-5}$	$(7.032 \pm 0.123) \times 10^{-7}$
3970.1	$(3.565 \pm 0.023) \times 10^{-5}$	$(3.441 \pm 0.048) \times 10^{-6}$
3889.1	$(3.817 \pm 0.024) \times 10^{-5}$	$(3.164 \pm 0.045) \times 10^{-6}$
3835.4	$(3.517 \pm 0.022) \times 10^{-5}$	$(1.881 \pm 0.029) \times 10^{-6}$
3797.9	$(4.438 \pm 0.024) \times 10^{-5}$	$(3.892 \pm 0.047) \times 10^{-6}$
3770.1	$(5.428 \pm 0.023) \times 10^{-5}$	$(5.483 \pm 0.048) \times 10^{-6}$
3749.8	$(6.417 \pm 0.019) \times 10^{-5}$	$(5.666 \pm 0.034) \times 10^{-6}$
3570.0	$(1.000 \pm 0.019) \times 10^{-5}$	$(1.180 \pm 0.034) \times 10^{-6}$

NOTE.—The errors are the combined photon-statistics errors.

In the presence of any continuous emission, the relative line depth in the nebula $R_N = (C_N - L_N)/C_N$ is smaller than the relative line depth $R_S = (C_S - L_S)/C_S$ of the same line in the illuminating star, where C and L refer to continuum and line-center intensities, respectively, and where the subscripts N and S refer to the nebular and stellar spectrum, respectively. The fluorescence intensity relative to the scattered nebular continuum can therefore be expressed as $R_S/R_N - 1$ (see Witt & Vijh 2004 for a review).

Given the nature of our measuring technique, we can determine the fluorescence intensity only at the wavelengths of the resolvable Balmer lines as well as the Balmer discontinuity, i.e., at 10 wavelength positions with our spectral resolution in our spectral range. By measuring the line depths of each of the Balmer lines in the star and the nebula, we extracted the fluorescence intensities at those wavelengths. Table 1 shows the fluorescence intensities at the two offsets: 2.5 south, 3.9 east and 5" south, 6.5 east. Independent observations by the authors using the 90" Bok telescope (Steward Observatory) and the Boller & Chivens spectrograph show corroborating evidence for this UV/blue fluorescence in the RR (U. Vjih, A. Witt, & K. Gordon 2004, in preparation).

3.2. Identification

Hydrogenated amorphous carbon (HAC), silicon nanoparticles (SNP), SiC grains, and small PAHs are all known to luminesce at blue wavelengths and have also been considered as likely candidates to explain the ERE (Witt & Vjih 2004). The left panel of Figure 4 shows photoluminescence spectra of HAC, SNP, and SiC (Li et al. 2000; Huang et al. 2002; Liao et al. 2002; Belomoin, Therrien, & Nayfeh 2000; Patrone et al. 2000). It reveals that the observed blue luminescence (BL) in the RR is unlike the luminescence spectrum of HACs, SNPs, or SiC. Given the exceptionally strong UIR band emission in the RR, the most likely source of the newly discovered BL may then be fluorescence by PAH molecules. The nebular BL spectrum suggests a peak in the fluorescence intensity corresponding the first electronic transition $S_1 - S_0$ near 3750 Å. Comparison with Figure 1 suggests PAH molecules in the mass range of 170–270 amu as the likely sources. Shown in the right panel of Figure 4 are comparisons with laboratory fluorescence spectra (Chi et al. 2001a, 2001b; Reylé & Bréchnignac 2000) of gas-phase PAHs in that mass range with the BL spectrum of the RR at an offset of 2.5 south, 3.9 east.

Laboratory spectra obtained with PAHs in the gas phase are more likely to be comparable to astrophysical spectra. These gas-phase spectra show considerable variation with temperature, becoming smoother, losing band structure, and the peak

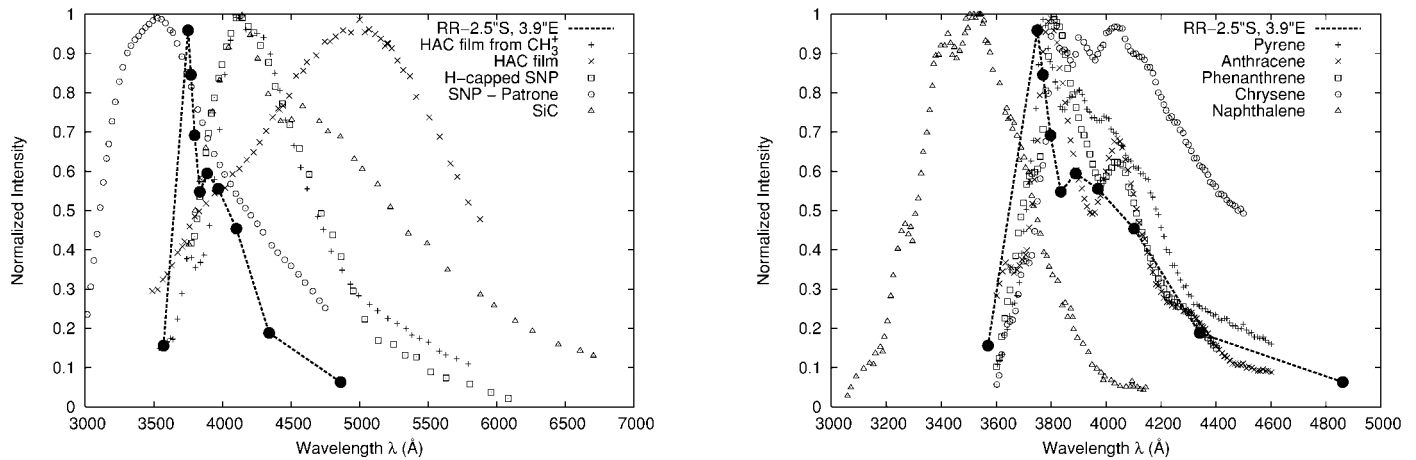


FIG. 4.—UV/blue fluorescence spectra of the RR nebula compared with PAH and solid-state luminescence. *Left*: Comparison with some solid-state candidates. *Right*: Comparison with small neutral PAHs. The intensities are normalized for easy comparison of the spectra with existing laboratory fluorescence spectra. The dotted lines representing the RR fluorescence spectrum are drawn to guide the eye (measurements exist only at specific wavelengths indicated by filled circles). [See the electronic edition of the *Journal* for a color version of this figure.]

shifting to longer wavelengths with increasing temperatures (Chi et al. 2001a, 2001b). Although anthracene suggests a good match to the observed spectrum, we do not have sufficient spectral resolution to completely rule out other possible candidates since the measurement technique works only at the discrete wavelengths of the Balmer lines.

4. DISCUSSION

Another important factor that should be considered when identifying possible carriers is fluorescence efficiency. Although many different fluorescing species may exist with similar abundances, the spectra of the most efficient ones will be dominant. Laboratory studies have shown that when comparing emission rates per molecule, from PAH molecules placed at 1 AU from the Sun, anthracene and pyrene show 10–100 times more efficiency than naphthalene ($C_{10}H_8$) and phenanthrene ($C_{14}H_{10}$)

(Bréchnignac & Hermine 1994). Additional support for small PAHs as sources of the observed BL is found in the spatial correlation between the BL and the PAH $3.3 \mu\text{m}$ emission in the RR and the presence of the distinct PAH ionization discontinuity in the spectrum of the central source, HD 44179 (U. Vijh, A. Witt, & K. Gordon 2004, in preparation).

We are grateful to David F. Malin for providing a rare blue image of the RR nebula. U. P. V. acknowledges a CTIO thesis student travel grant. This research was made possible through a generous allocation of observing time at CTIO and through grants from the US National Science Foundation and NASA. We would also like to thank Louis Allamandola for his valuable comments on the manuscript. We thank the anonymous referee for his/her comments that have significantly improved this Letter.

REFERENCES

- Allamandola, L. J., Tielens, A. G. G. M., & Barker, J. R. 1985, *ApJ*, 290, L25
 Belomoin, G., Therrien, J., & Nayfeh, M. 2000, *Appl. Phys. Lett.*, 77, 779
 Berlman, I. B. 1965, *Handbook of Fluorescence Spectra of Aromatic Molecules* (New York: Academic Press)
 Bréchnignac, P., & Hermine, P. 1994, in *AIP Conf. Proc. 312, Molecules and Grains in Space*, ed. I. Nenner (New York: AIP), 613
 Bujarrabal, V., Neri, R., Alcolea, J., & Kahane, C. 2003, *A&A*, 409, 573
 Chi, Z., Cullum, B. M., Stokes, D. L., Mobley, J., Miller, G. H., Hajaligol, M. R., & Vo-Dinh, T. 2001a, *Spectrochem. Acta A*, 57, 1377
 ———. 2001b, *Fuel*, 80, 1819
 Cohen, M., et al. 1975, *ApJ*, 196, 179
 Cook, D. J., & Saykally, R. J. 1998, *ApJ*, 493, 793
 Ewald, M., & Garrigues, Ph. 1985, in *Spectral Atlas of Polycyclic Aromatic Compounds*, ed. W. Karcher et al. (Dordrecht: Kluwer), 34
 ———. 1988, in *Spectral Atlas of Polycyclic Aromatic Compounds*, Vol. 2, ed. W. Karcher et al. (Dordrecht: Kluwer), 58
 Geballe, T. R., Lacy, J. H., Persson, E. E., McGregor, P. J., & Soifer, B. T. 1985, *ApJ*, 292, 500
 Hony, S., et al. 2001, *A&A*, 370, 1030
 Huang, X., Xu, J., Li, W., & Chen, K. 2002, *Thin Solid Films*, 422, 130
 Jochims, H. W., Baumgaertel, H., & Leach, S. 1999, *ApJ*, 512, 500
 Keller, R. 1987, in *Polycyclic Aromatic Hydrocarbons and Astrophysics*, ed. A. Léger, L. d'Hendecourt, & N. Boccara (NATO ASI Ser. C, 191; Dordrecht: Kluwer), 387
 Leger, A., & Puget, J. L. 1984, *A&A*, 137, L5
 Li, G., Burggraf, L. W., Shoemaker, J. R., Eastwood, D., & Steigman, A. E. 2000, *Appl. Phys. Lett.*, 76, 3373
 Liao, M., Feng, Z., Chai, C., Yang, S., Liu, Z., & Wang, Z. 2002, *J. Appl. Phys.*, 91, 1891
 Patrone, L., Nelson D., Safarov, V., Sentis, M., Marine, W., & Giorgio, S. 2000, *J. Appl. Phys.*, 8, 205
 Peaden, P. A., Lee, M. L., Hirata, Y., & Novotny, M. 1980, *Anal. Chem.*, 52, 2268
 Peeters, E., Allamandola, L. J., Hudgins, D. M., Hony, S., & Tielens, A. G. G. M. 2004, in *ASP Conf. Ser. 309., Astrophysics of Dust*, ed. A. N. Witt, G. C. Clayton, & B. T. Draine (San Francisco: ASP), in press (astro-ph/0312184)
 Reylé, C., & Bréchnignac P. 2000, *European J. Phys. D*, 8, 205
 Russell, R. W., Soifer, B. T., & Willner, S. P. 1978, *ApJ*, 220, 568
 Schmidt, G. D., & Witt, A. N. 1991, *ApJ*, 383, 698
 Sellgren, K. 1984, *ApJ*, 277, 623
 Snow, T. P., & Witt, A. N. 1995, *Science*, 270, 1455
 van Winckel, H. 2003, *ARA&A*, 41, 391
 Verstraete, L., et al. 2001, *A&A*, 372, 981
 Whittet, D. C. B. 2003, *Dust in the Galactic Environment* (2nd ed.; Bristol: IoP)
 Witt, A. N., & Boroson, T. A. 1990, *ApJ*, 355, 182
 Witt, A. N., & Vijh, U. P. 2004, in *ASP Conf. Ser. 309, Astrophysics of Dust*, ed. A. N. Witt, G. C. Clayton, & B. T. Draine (San Francisco: ASP), in press (astro-ph/0309674)